NANO-MICRO LETTERS ARTICLE
www.nmletters.org

A Novel Photothermal Nanocrystals of Cu_7S_4 Hollow Structure for Efficient Ablation of Cancer Cells

Guosheng Song[1,†], Linbo Han[1,2,†], Weiwei Zou[3,*], Zhiyin Xiao[1], XiaoJuan Huang[1], Zongyi Qin[1], Rujia Zou[1], Junqing Hu[1,*]

(Received 31 December 2013; accepted 18 February 2014; published online 20 March 2014)

Abstract: $Cu_{2-x}S$ nanocrystals (NCs), characterized by low cost, low toxicity, high stability and high photothermal conversion efficiency, provide promising platforms as photothermal agents. Herein, a novel two-step synthesis has been developed for Cu_7S_4 nanocrystals with hollow structure using the as-prepared copper nanoparticles as starting a solid precursor followed by hot-injection of sulfide source.The Cu_7S_4 NCs exhibit intense absorption band at Near-infrared (NIR) wavelengths due to localized surface plasmon resonance (LSPR) mode, which can effectively convert 980 nm-laser energy into heat.Moreover, the localized high temperature created by Cu_7S_4 NCs under NIR irradiation could result in efficient photothermal ablation (PTA) of cancer cells *in vivo*, demonstrating a novel and promising photothermal nanomaterials.
Keywords: Semiconductor nanocrystals; Near-infrared absorption; Photothermal

Citation: Guosheng Song, Linbo Han, Weiwei Zou, Zhiyin Xiao, XiaoJuan Huang, Zongyi Qin, Rujia Zou and Junqing Hu, "A Novel Photothermal Nanocrystals of Cu_7S_4 Hollow Structure for Efficient Ablation of Cancer Cells", Nano-Micro Lett. 6(2), 169-177 (2014). http://dx.doi.org/10.5101/nml.v6i2.p169-177

Introduction

Near-infrared (NIR)-laser-driven photothermal ablation (PTA) therapy has attracted great attention in recent years as a minimally invasive and potentially more effective treatment alternative to conventional approaches [1-16]. In order to promote the photothermal conversion efficiency and gain access to efficient PTA therapy, it is the developing novel photothermal conversion agents that we are focusing on.Currently, four types of photothermal agents have been extensively developed in PTA therapy. The first type are organic compounds (e.g., indocyanine green (ICG) dye [1] and poly aniline nanoparticles [2]), which may suffer from limitations such as photobleaching or unsatisfactory photothermal conversion efficiency. The second type are carbon nanomaterials (including carbon nanotubes [3-5] and graphene [6-9]) whose absorption coefficient in the NIR region is usually not as high as expected. The third type are noble metal nanostructures, such as nanorods [10-12], nanoshells [13,14], nanocages [15,16], nanostars [17] and Pd- nanosheets [18].

These noble metal nanostructures exhibit intense NIR photoabsorption, and also are the most widely explored kind of photothermal agents. However, their practical applications are limited by the high cost. Alternatively, copper-containing semiconductor nanocrystals, characterized by low production cost, high stability, low toxicity, and high photothermal conver-

[1]State Key Laboratory for Modification of Chemical Fibers and Polymer Materials, College of Materials Science and Engineering, Donghua University, Shanghai 201620, China
[2]Department of Chemical and Materials Engineering, University of Alberta, Edmonton, Alberta, T6G2V4, Canada
[3]Radiology Departments, Changzheng Hospital, Shanghai 200003, China
[†]These authors contributed equally to this work.
*Corresponding author. E-mail: czyyzww@163.com, hu.junqing@dhu.edu.cn

sion efficiency, provide promising platforms as photothermal agents [19-23]. CuS nanoparticles [24], CuS superstructures [21], Cu_9S_5nanocrystals [19], and Fe_3O_4@$Cu_{2-x}S$ [22], Cu_9S_5@SiO_2 [20] nanocomposites have been developed as 980 nm laser-driven photothermal agents for efficient PTA of cancer cells *in vitro* and *in vivo*. To meet the severe requirements of future PTA therapy, it is still necessary to develop novel kind of copper chalcogenides based photothermal agents. Herein, we have developed a novel two-step method for preparation of Cu_7S_4 nanocrystals with hollow structure and investigated them as a potential of 980 nm-laser-driven photothermal agents.

Experimental

Characterization: Sizes, morphologies, and microstructures of the samples were determined by field emission transmission electron microscope (TEM, JEOL, JEM-2100F). Powder X-ray diffraction (XRD) was conducted by a D/max-2550 PCX-ray diffract meter (Rigaku, Japan). UV-Vis-NIR absorption spectra were measured on a UV-2550 Spectrophotometer (Shimadzu, Japan).

Synthesis of Cu_7S_4 NCs: All of the chemicalswere bought from Aladdin and are analytically pure, which were used as received without further purification. The preparation of copper NCs followed a modified procedure [25]. Briefly, 0.5 mmol of copper acetylacetonate was dissolved in 15 mL of oleylamine in a 100 mL flask, which was purged with dry nitrogen gas to remove residual water and oxygen. The reaction mixture was heated to 230°C at a rate of 5°C /min by a heating mantle while being magnetically stirred and then kept at 230°C for 10 min to form copper NCs. Subsequently, a certain amount of sulfur (e.g. 0 mmol, 0.1 mmol, 0.2 mmol, 0.3 mmol, 0.5 mmol and 0.6 mmol) dissolved in 5 mL of oleylamine was quickly injected into the solution. The resulting mixture was maintained at 230°C for 30 min. After the solution was cooled to room temperature, the Cu_7S_4 NCs were purified by washing with n-hexane. Subsequently, the Cu_7S_4 NCs dispersed into 15 mL of chloroform for later use.

Synthesis of polymer-modified Cu_7S_4 NCs: The as-prepared Cu_7S_4 NCs were coated with an amphiphilic hydrolyzed poly (maleic anhydride) pre-modified with dodecylamine according to a literature report [23,28]. In a 50 mL round bottom flask, 530 μL of the amphiphilic polymer stock solution (0.8 M monomer units in $CHCl_3$), 5 mL of the above Cu_7S_4 NCs chloroform solution and 25 mL of anhydrous $CHCl_3$ were combined and vortexed with magnetically stirring for 45 minutes at room temperature. Subsequent rotary evaporation of the solvent resulted in a dark-brown film of polymer coated Cu_7S_4 NCs attached to the inner wall of the flask. 10 mL of aqueous sodium borate buffer (SBB, pH12) was then added to the flask and subject to ultrasonication for 15 min. After phase transfer from chloroform to aqueous solution, the hydrophilic Cu_7S_4 NCs were collected by centrifugation. The aqueous solution of the Cu_7S_4 NCs was stored at 4°C for later use.

Measurement of photothermal performance: A 980 nm laser was delivered through a quartz cuvette containing aqueous dispersion (0.3 mL) of the aqueous solution containing Cu_7S_4NCs with different concentrations (i.e., 6.25, 12.5, 25, 50, 80, 100 and 150 μg/mL). The light source was an external adjustable power (0-0.8 W) 980 nm semiconductor laser device laser module (Xi'an Tours Radium Hirsh Laser Technology Co., Ltd. China). The output power density was independently calibrated to be 0.72 W/cm^2 using a handy optical power meter (Newport model 1918-C, CA, USA). A thermocouple with an accuracy of 0.1°C was inserted into the aqueous dispersion of Cu_7S_4NCs, which was oriented perpendicular to the path of the laser beam. The temperature was recorded one time per 5 s.

In vitro cytotoxicity of Cu_7S_4 NCs

Hepatocarcinoma cell lines Hep3B cells were seeded in a 96-well plate at a density of 1×10^4 cells/well for 24 h at 37°C in 5% CO_2 to allow the cells to attach. The culture medium was changed and cells were incubated with complete medium containing the Cu_7S_4 NCsat a series of concentrations (i.e., 50, 100, 150, 200 and 250 μg/mL) at 37°C with 5% CO_2 for further 24 h. After that, 0.1 mL of 3-(4,5)-dimethylthiahiazo-2-yl)-2,5-diphenyltetrazolium bromide (MTT) solution (5 mg/mL, Sigma, Cat.M2003) was added to each well of the microtiter plate and then was incubated in the CO_2 incubator for 4 h. The cells then were lysed by the addition of 100 μL of dimethylsulfoxide (DMSO). The spectrophotometric absorbance of formazan was measured using a plate reader at 570 nm. Four replicates were done for each treatment group.

In vivo photothermal ablation of cancer cells

Severe combined immunodeficiency (SCID) mice were inoculated subcutaneously with 4×10^6 hepatocarcinoma cell lines Hep3B cells on the left side of the rear leg 4-5 weeks before the experiments. When tumors grew to 8-12 mm in diameter, the SCID mice were randomly labeled as control and treatment sample. Two nude mice were first anaesthetized by trichloroacetaldehyde hydrate (10%) at a dosage of 40 mg/kg body weight, and then the treatment and control were injected with 0.15 mL of PBS solution containing the Cu_7S_4 NCs (150 μg/mL) and saline, respectively, at

the central region of the tumors with a depth of ~4 mm. After 2 h, the tumors of the control and treatment group were irradiated with 980 nm laser (an output power density of 0.72 W/cm^2) for 10 min. After that, the two SCID mice were scarified and tumors were removed, embedded in paraffin, and cryosectioned into 4 μm slices. These slides were stained with hematoxylin/eosin, the nexamined under a Zeiss Axiovert 40 CFL inverted fluorescence microscope, and images were captured with a Zeiss AxioCam MRc5 digital camera.

Results and discussion

Cu_7S_4nanocrystals (NCs) were synthesized by a two-step method, as shown in Fig. 1. Asa first step, copper nanoparticles were synthesized using oleylamine as reducing agents, according to reported method [25]. Then the as-prepared copper nanoparticles were used as solid precursor, which could react with sulfide source introduced by hot-injection. As a result, the hollow-structure Cu_7S_4 NCs could be successfully fabricated.

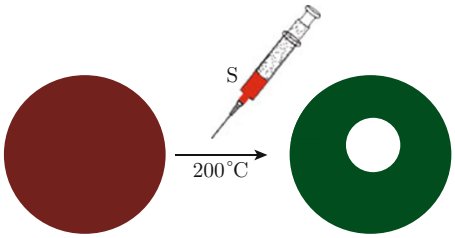

Fig. 1 Schematic illustration of the preparation step of Cu_7S_4 NCs with hollow structure.

The copper nanoparticles were prepared without injection of sulfide source (e.g. 0 g). Figure 2(a) showed the typical transmission microscopy (TEM) image of the copper nanoparticles. The particles are spherical and have an average diameter of 15 nm. The high magnification of TEM images (Fig. S1) showed that the copper nanoparticle was crystalline with a certain amount of surface oxidation. As the copper nanoparticle show a high activity to react with oxygen [25], the oxidation likely occurred before XRD measurement when the specimen was exposed to air. Therefore, the crystalline structures of the copper nanoparticles were indexed to CuO (JCPDS card No. 44-0706), as shown in Fig. S3. The resulting UV-vis spectrum of the copper nanoparticles (Fig. S2) exhibited a well-defined surface plasmon absorption peak occurred at around 580 nm, which was consistent with previous reports, confirming the successful synthesis of copper nanoparticles [25].

The resultant copper nanoparticles with a uniform diameter could be used as a sacrificial solid precursor for the synthesis of Cu_7S_4NCs with hollow structure by injection of an appropriate sulfide source (e.g. 0.6 mmol). Compared to copper seeds synthesized from the first step (Fig. 2(a)), the diameter of Cu_7S_4 NCs, after 30 min aging of the second injection of sulfide source, were within an average size of 15-30 nm, as shown in Fig. 2(b). Moreover, the solid nanoparticles were converted into some hollow structures, as shown in high magnification of TEM (Fig. 2(c) and 2(d)). This hollowing process could be explained by the Kirk end all diffusion [26]. The diffraction peaks of the hollow nanoparticles prepared with the S source of 0.6 mmol (Fig. 3) could be indexed with those of Cu_7S_4 (JCPDS

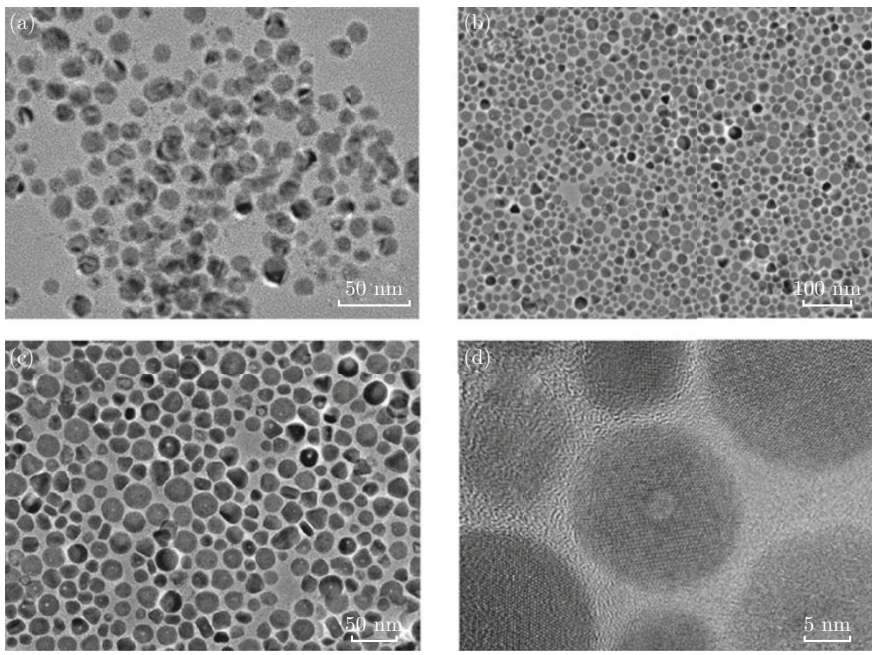

Fig. 2 (a) TEM images of copper nanoparticles; ((b), (c) and (d)) TEM and high magnification of TEM images of Cu_7S_4 NCs prepared with the sulfide source of 0.6 mmol.

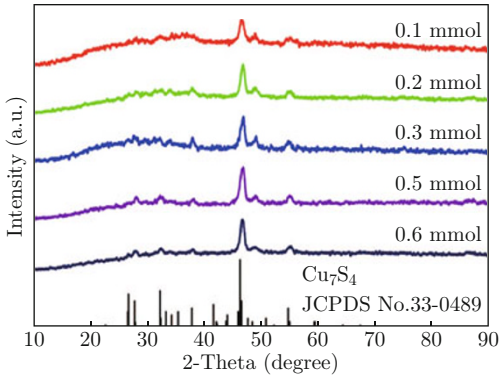

Fig. 3 XRD of the Cu_7S_4 NCs prepared with different sulfide source (e.g. 0.1 mmol, 0.2 mmol, 0.3 mmol, 0.5 mmol and 0.6 mmol).

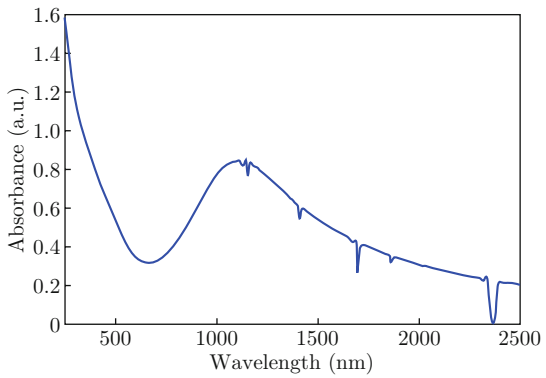

Fig. 4 UV-Vis-NIR absorbance spectrum of chloroform solution containing the Cu_7S_4 NCs prepared with the sulfide source of 0.6 mmol.

card No. 33-0489), confirming the successful preparation of Cu_7S_4.

Encouragingly, the Cu_7S_4NCs dissolved in chloroformshowed an intense absorption band in NIR region owing to the localized surface plasmon resonance (LSPR) mode, as shown in Fig. 4. Specifically, the Cu_7S_4NCs exhibit a minimum of absorption around ~670 nm and an increased absorption with the increase of wavelength with the maximum absorption peak of ~1100 nm, in analogy to the reported $Cu_{2-x}S$ [19,24]. This stronger absorption in NIR region of Cu_7S_4 NCs prepared by injecting sulfide source makes them a potential 980 nm-laser-driven photothermal agents for ablation of cancer cells.

We also investigated the effect of sulfide amount on crystal structure and morphology of copper sulphide nanoparticles. The resultant copper nanoparticles, as sacrificial templates, were used to react with sulfide source with different doses (e.g. 0.1 mmol, 0.2 mmol, 0.3 mmol and 0.5 mmol). The corresponding X-ray diffraction (XRD) patternswere displayed in Fig. 3. The diffraction peaks of all as-prepared Cu_7S_4 NCs could be indexed with those of Cu_7S_4 (JCPDS card No. 33-0489), confirming the successful preparation of Cu_7S_4. According to the previous literatures, there are at least five stable phases for the $Cu_{2-x}S$ system (i.e., covellite CuS, anilite $Cu_{1.75}S$, digenite $Cu_{1.8}S$, djurlite $Cu_{1.95}S$, and chalcocite Cu_2S) [19,21,27]. In the present study, we are able to obtain ananilite Cu_7S_4

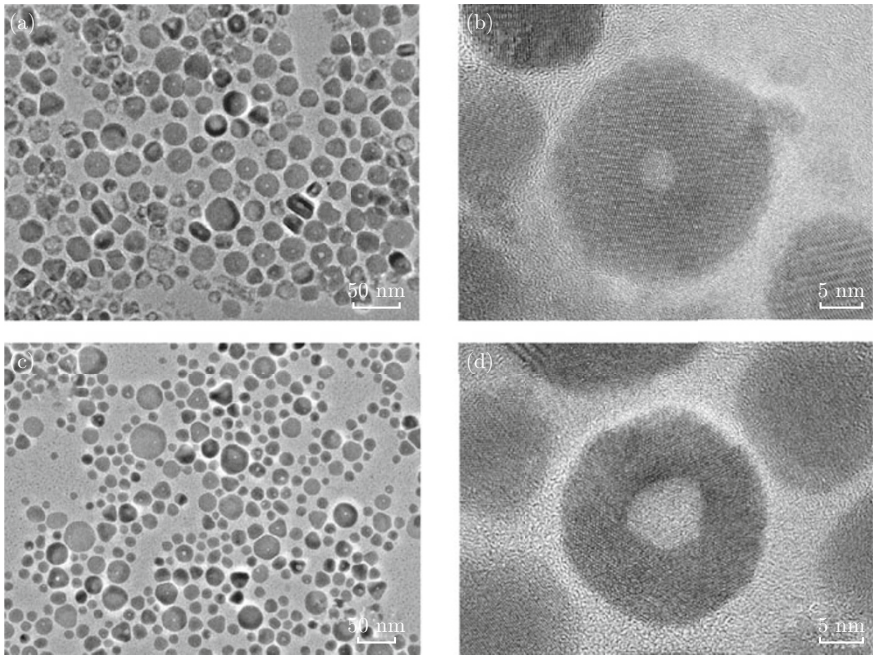

Fig. 5 TEM images and high magnification of TEM of Cu_7S_4 NCs prepared with the sulfide source of ((a), (b)) 0.1 mmol, ((c), (d)) 0.2 mmol, respectively.

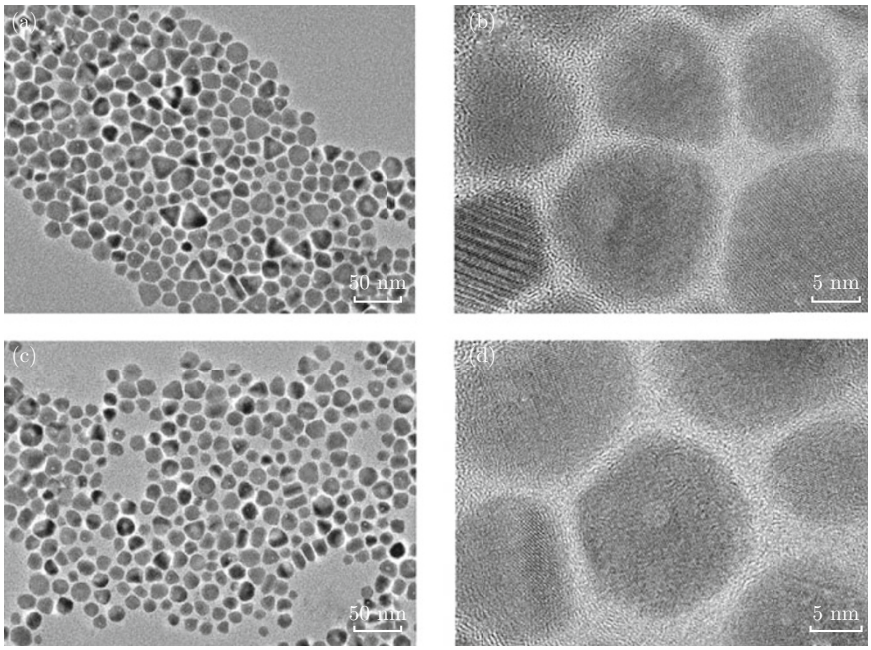

Fig. 6 TEM images and high magnification of TEM of Cu_7S_4 NCs prepared with the sulfide source of ((a), (b)) 0.3 mmol, ((c), (d)) 0.5 mmol, respectively.

nanocrystals (orthorhombic, space group P62/nma JCPDS No.33-0489) from Cu nanoparticles by injecting of different doses of sulfide source. It seems that the amount of sulfide source has no obvious effect on the crystal structure of final product. It should also be noted that the difference in morphology and size can be largely dependent on the amount of sulfide source. When adding 0.1 mmol of sulfide source, the obtained nanocrystals with spherical shape and relatively uniform diameter of 25 nm, as shown in Fig. 5(a) and 5(b). With the increase of the sulfide source from 0.1 mmol to 0.2 mmol, the uniformity of size decreased. Specifically, two obvious different sizes (including average diameter 15 and 35 nm) of nanocrystals coexisted in the final product, as shown in Fig. 5(c). Moreover, the nanoparticles exhibit obvious hollow structure, as shown in Fig. 5(d). Further increase of sulfide source to 0.3 mmol resulted in more triangular morphology existing in the product as shown in Fig. 6(a) and 6(b). Besides, 0.5 mmol of sulfide source could lead to less obviously hollow core structure in final products as show in Fig. 6(c) and 6(d).

Due to their strong absorption in NIR region, the Cu_7S_4 NCs prepared with 0.6 mmol of sulfide source were chosen as an example to investigate the photothermal conversion performance and the potential as 980 nm-laser-driven photothermal agents. The as-synthesized Cu_7S_4 NCs were passivated with oleylamine and could not be dispersed into aqueous or physiological solution, which limited these nanocrystals applying directly to biologicalsystem.To obtain hydrophilic Cu_7S_4 NCs, an amphiphilic polymer was coated on the surface of Cu_7S_4 NCs by hydrophobic self-assembly [23,28]. The polymer-modified Cu_7S_4 NCs could be easily dispersed in water or phosphate buffered saline (PBS) at pH 7.4.

The photothermal conversion performance of the Cu_7S_4 NCs was examined under the irradiation of 980 nm laser with power density of 0.72 W/cm^2 by detecting the extent of temperature increase, as shown in Fig. 7. Pure water was used as a negative control. The temperatures of all the Cu_7S_4 NCs increased with the irradiation time, and the temperature increased more rapidly with increasing the concentration of Cu_7S_4 NCs. The temperature of Cu_7S_4 NCs aqueous dispersion (e.g. 150 μg/mL) could be elevated by 15.7°C with the irritation of 980 nm laser for 400 s, compared with pure water (i.e., 0 μg/mL) that was only increased by less than 4°C. These confirmed the Cu_7S_4 NCs can rapidly and efficiently convert the 980 nm-laser energy into thermal energy. Moreover, with the increase of the concentration (i.e., from 6.25 to 12.5, 25, 50, 80 and 100 μg/mL), the temperature of the Cu_7S_4 NCs aqueous dispersion could be increased by 6.5, 8, 8.7, 10.1, 12.2 and 14.1°C, respectively (Fig. 7(b)). As is well-known, hyperthermic therapy takes advantage of heat between 40 and 45°C to damage cancer cells [29]. Assuming that the temperature of *in vivo* human body is 37°C, tumor region injected with an aqueous dispersion of Cu_7S_4 NCs can easily be heated to over 45°C within 400 s by irradiation with a 980 nm laser (0.72 W/cm^2), which probably efficiently induces cancer cells death [29].

The influence of the Cu_7S_4 NCs on the viabilities of cancer cells were used to evaluate the biocompatibility

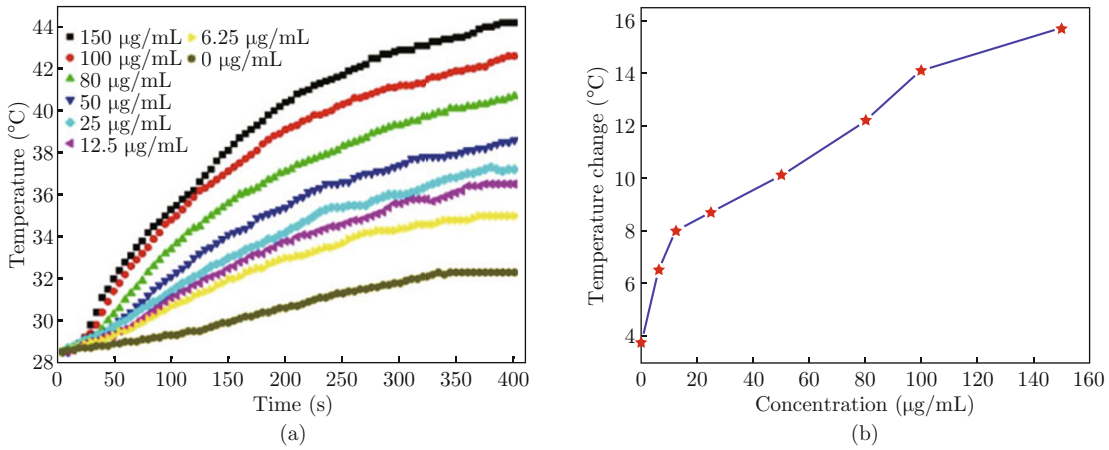

Fig. 7 Temperature elevation of the aqueous solution containing Cu_7S_4 NCs with different concentrations (i.e., 6.25, 12.5, 25, 50, 80, 100 and 150 μg/mL) as a function of time (0-400 s) under the irradiation of 980 nm laser with power density of 0.72 W/cm^2; (b) Plot of temperature change over a period of 400 s versus the aqueous dispersion of the Cu_7S_4 NCs.

in vitro. The Cu_7S_4 NCs with various concentrations (i.e., 50, 100, 150, 200 and 250 μg/mL) were incubated with Hepatocarcinoma cell lines Hep3B cells for 24 h and then the cell viabilities were tested by using the 3-(4,5-dimethylthiazol-2-yl)-2,5-diphenyltetrazolium bromide (MTT) assay. There was no obvious adverse effect on cell viabilities, even the concentration reaching 250 μg/mL, as shown in Fig. 8, which meant a low cytotoxicity induced by Cu_7S_4 NCs.

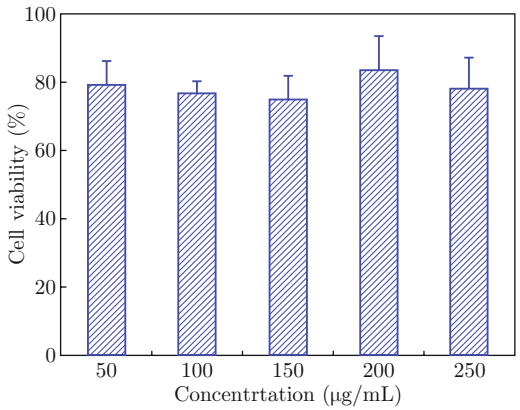

Fig. 8 The viabilities of Hep3B cells incubated with the Cu_7S_4 NCs with different concentrations (i.e., 50, 100, 150, 200 and 250 μg/mL) for 24 h, measured by MTT assay. Data represents the mean±standard deviation of four experiments.

To evaluate photothermal ablation effect of cancer cells, two nude mice bearing evident tumors were randomly divided into control and treatment group. The control mouse was injected with 200 μL of saline in the central region of the tumor, while the treatment mouse was injected with 200 μL of PBS containing Cu_7S_4 NCs (e.g., 150 μg/mL). After 2 h, the tumors of the two mice were irradiated with 980 nm of laser for 10 min (see detail in experiment section and the experimental setup shown in Fig. S4). Subsequently, PTA effects of tumor tissues in mice were confirmed by histological examination (hematoxylin/eosin (H&E) staining), as shown in Fig. 9. In the case of control group, there were little change regarding the cells' sizes and shapes, nuclear modifications as shown in Fig. 9(a) and 9(c). In the case of treatment group, under the same irradiation conditions, the common signs of thermal cell necrosis are presented on considerable regions of the examined tumor slide (Fig. 9(b)). Furthermore, more destruction of the tumor cells, such as shrinkage of the malignant cells, loss of contact, eosinophilic cytoplasm, and nuclear damage could be observed from Fig. 9(d). These facts suggested that *in vivo* cancer cells could be efficiently destroyed by the high temperature arising from the excellent photothermal effect of Cu_7S_4 NCs. Therefore, it is safe to conclude that Cu_7S_4 NCs have great potential to be used as an excellent photothermal agent for PTA therapy.

Conclusion

Using the copper nanoparticles as a starting precursor, we have successfully synthesized Cu_7S_4 NCs with hollow structure, which exhibited intense absorption band at NIR wavelengths due to LSPR. The hydrophilic Cu_7S_4 NCs coated with amphiphilic polymer could effectively convert 980 nm-laserenergy into heat and further destroy cancel cells *in vivo*. Therefore, these Cu_7S_4 hollow NCs demonstrated great superiority as an excellently potential photothermal agent, as a result of their small size and high photothermal conversion efficiency as well as their low cost.

Acknowledgements

This work was financially supported by the National

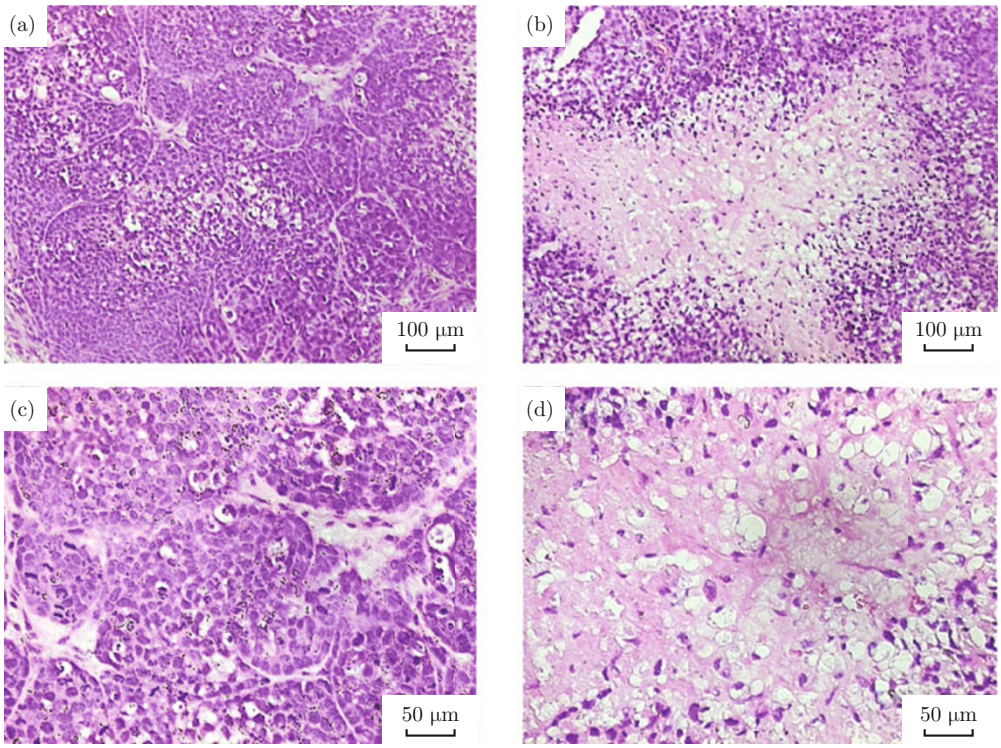

Fig. 9 (a)-(d) Representative H&E stained histological images of *in vivo* tumor sections treated by the irradiation of 980 nm laser (0.72 W/cm^2) over a period of 10 min injected with ((a), (c)) saline and ((b), (d)) PBS solution of the Cu_7S_4 NCs (150 μg/mL), respectively.

Natural Science Foundation of China (Grant Nos. 21171035 and 51302035), the Key Grant Project of Chinese Ministry of Education (Grant No. 313015), the PhD Programs Foundation of the Ministry of Education of China (Grant Nos. 20110075110008 and 20130075120001), the National 863 Program of China (Grant No. 2013AA031903), the Science and Technology Commission of Shanghai Municipality (Grant No. 13ZR1451200), the Fundamental Research Funds for the Central Universities, the Hong Kong Scholars Program, the Program for Changjiang Scholars and Innovative Research Team in University (Grant No. IRT1221), the Shanghai Leading Academic Discipline Project (Grant No. B603), and the Program of Introducing Talents of Discipline to Universities (No. 111-2-04).

References

[1] J. Yu, D. Javier, M. A. Yaseen, N. Nitin, R. Richards-Kortum, B. Anvari and M. S. Wong, "Self-assembly synthesis, tumor cell targeting, and photothermal capabilities of antibody-coated indocyanine green nanocapsules", J. Am. Chem. Soc. 132(6), 1929-1938 (2010). http://dx.doi.org/10.1021/ja908139y

[2] J. Yang, J. Choi, D. Bang, E. Kim, E. K. Lim, H. Park, J. S. Suh, K. Lee, K. H. Yoo, E. K. Kim, Y. M. Huh and S. Haam, "Convertible organic nanoparticles for near-infrared photothermal ablation of cancer cells", Angew. Chem. Int. Ed. 50(2), 441-444 (2011). http://dx.doi.org/10.1002/anie.201005075

[3] X.Wang, C.Wang, L.Cheng, S.-T. Lee and Z. Liu, "Noble metal coated single-walled carbon nanotubes for applications in surface enhanced raman scattering imaging and photothermal therapy", J. Am. Chem. Soc. 134(17), 7414-7422 (2012). http://dx.doi.org/10.1021/ja300140c

[4] V.S.Thakare, M.Das, A. K. Jain, S.Patil and S. Jain, "Carbon nanotubes in cancer theragnosis", Nanomedicine 5(8), 1277-1301 (2010). http://dx.doi.org/10.2217/nnm.10.95

[5] F. Zhou, S. Wu, S. Song, W. R. Chen, D. E. Resasco and D. Xing, "Antitumor immunologically modified carbon nanotubes for photothermal therapy", Biomaterials 33(11), 3235-3242 (2012). http://dx.doi.org/10.1016/j.biomaterials.2011.12.029

[6] J. T. Robinson, S. M. Tabakman, Y. Liang, H. Wang, H. S. Casalongue, V. Daniel and H. Dai, "Ultrasmall reduced graphene oxide with high near-infrared absorbance for photothermal therapy", J. Am. Chem. Soc. 133(17), 6825-6831 (2011). http://dx.doi.org/10.1021/ja2010175

[7] M. Li, X. Yang, J.Ren, K.Qu and X. Qu, "Using graphene oxide high near-infrared absorbance for photothermal treatment of alzheimer's disease", Adv. Mater. 24(13), 1722-1728 (2012). http://dx.doi.org/10.1002/adma.201104864

[8] K. Yang, L. Hu, X. Ma, S. Ye, L. Cheng, X. Shi, C. Li, Y. Li and Z. Liu, "Multimodal imaging guided

photothermal therapy using functionalized graphene nanosheets anchored with magnetic nanoparticles", Adv. Mater. 24(14), 1868-1872 (2012). http://dx.doi.org/10.1002/adma.201104964

[9] K. Yang, J. Wan, S. Zhang, B. Tian, Y. Zhang and Z. Liu, "The influence of surface chemistry and size of nanoscale graphene oxide on photothermal therapy of cancer using ultra-low laser power", Biomaterials. 33(7), 2206-2214 (2012). http://dx.doi.org/10.1016/j.biomaterials.2011.11.064

[10] B. Jang, J. Y. Park, C. H. Tung, I. H. Kim and Y. Choi, "Gold nanorod-photosensitizer complex for near-infrared fluorescence imaging and photodynamic/photothermal therapy *in vivo*", ACS Nano. 5(2), 1086-1094 (2011). http://dx.doi.org/10.1021/nn102722z

[11] C. G. Wang, J. Chen, T. Talavage and J. Irudayaraj, "Gold nanorod/Fe_3O_4nanoparticle nano-pearl-necklaces for simultaneous targeting, dual-mode imaging, and photothermal ablation of cancer cells", Angew. Chem. Int. Ed. 48(15), 2759-2763 (2009). http://dx.doi.org/10.1002/anie.200805282

[12] Z. Zhang, L. Wang, J. Wang, X. Jiang, X. Li, Z. Hu, Y. Ji, X. Wu and C. Chen, "Mesoporous silica-coated gold nanorods as a light-mediated multifunctional theranostic platform for cancer treatment", Adv. Mater. 24(11), 1418-1423 (2012). http://dx.doi.org/10.1002/adma.201104714

[13] H. Liu, T. Liu, X. Wu, L. Li, L. Tan, D. Chen and F. Tang, "Targeting gold nanoshells on silica nanorattles: a drug cocktail to fight breast tumors via a single irradiation with near-infrared laser light", Adv. Mater. 24(6), 755-761 (2012). http://dx.doi.org/10.1002/adma.201103343

[14] H. Liu, D. Chen, L. Li, T. Liu, L. Tan, X. Wu and F. Tang, "Multifunctional gold nanoshells on silica nanorattles: aplatform for the combination of photothermal therapy and chemotherapy with low systemic toxicity", Angew. Chem. Int. Ed. 50(4), 891-895 (2011). http://dx.doi.org/10.1002/anie.201002820

[15] Y. Xia, W. Li, C. M. Cobley, J. Chen, X. Xia, Q. Zhang, M. Yang, E. C. Cho and P. K. Brown, "Gold nanocages: from synthesis to theranostic applications", Acc. Chem. Res. 44(10), 914-924 (2011). http://dx.doi.org/10.1021/ar200061q

[16] J. Chen, C. Glaus, R. Laforest, Q. Zhang, M. Yang, M. Gidding, M. J. Welch and Y. Xia, "Gold nanocages as photothermal transducers for cancer treatment", Small 6(7), 811-817 (2010). http://dx.doi.org/10.1002/smll.200902216

[17] H.Yuan, A.M.Fales and T. Vo-Dinh, "TAT peptide-functionalized gold nanostars: enhanced intracellular delivery and efficient NIR photothermal therapy using ultralow irradiance", J. Am. Chem. Soc. 134 (28), 11358-11361 (2012). http://dx.doi.org/10.1021/ja304180y

[18] X. Q. Huang, S. H. Tang, X. L. Mu, Y. Dai, G. X. Chen, Z. Y. Zhou, F. X. Ruan, Z. L. Yang and N. F. Zheng, "Freestanding palladium nanosheets with plasmonic and catalytic properties", Nat. Nanotechnol.. 6(1), 28-32 (2011). http://dx.doi.org/10.1038/nnano.2010.235

[19] Q. Tian, F. Jiang, R. Zou, Q. Liu, Z. Chen, M. Zhu, S. Yang, J. Wang, J. Wang and J. Hu, "Hydrophilic Cu_9S_5nanocrystals: aphotothermal agent with a 25.7% heat conversion efficiency for photothermal ablation of cancer cells *in vivo*", ACS Nano 5(12), 9761-9771 (2011). http://dx.doi.org/10.1021/nn203293t

[20] G. Song, Q. Wang, Y. Wang, G. Lv, C. Li, R. Zou, Z. Chen, Z. Qin, K. Huo, R. Hu and J. Hu, "A low-toxic multifunctional nanoplatform based on Cu_9S_5@mSiO_2core-shell nanocomposites: combining photothermal- and chemotherapies with infrared thermal imaging for cancer treatment", Adv. Funct. Mater. 23(35), 4281-4292 (2013). http://dx.doi.org/10.1002/adfm.201203317

[21] Q. Tian, M.Tang, Y. Sun, R.Zou, Z.Chen, M.Zhu, S. Yang, J.Wang, J.Wang and J. Hu, "Hydrophilic flower-like CuS superstructures as an efficient 980 nm laser-driven photothermal agent for ablation of cancer cells", Adv. Mater. 23(31), 3542-3547 (2011). http://dx.doi.org/10.1002/adma.201101295

[22] Q. Tian, J. Hu, Y. Zhu, R. Zou, Z. Chen, S. Yang, R. Li, Q. Su, Y. Han and X. Liu, "Sub-10 nm Fe_3O_4@$Cu_{2-x}S$ core-shell nanoparticles for dual-modal imaging and photothermal therapy", J. Am. Chem. Soc. 135(23), 8571-8577 (2013). http://dx.doi.org/10.1021/ja4013497

[23] C. M. Hessel, V. P. Pattani, M. Rasch, M. G. Panthani, B. Koo, J. W. Tunnell and B. A. Korgel, "Copper selenide nanocrystals for photothermal therapy", Nano Lett. 11(6), 2560-2566 (2011). http://dx.doi.org/10.1021/nl201400z

[24] M. Zhou, R. Zhang, M. A. Huang, W. Lu, S. L. Song, M. P. Melancon, M. Tian, D. Liang and C. Li, "A chelator-free multifunctional [^{64}Cu]CuS nanoparticle platform for simultaneous micro-PET/CT imaging and photothermal ablation therapy", J. Am. Chem. Soc. 132(43), 15351-15358 (2010). http://dx.doi.org/10.1021/ja106855m

[25] M. Shi, H. S. Kwon, Z. Peng, A. Elder and H. Yang, "Effects of surface chemistry on the generation of reactive oxygen species by copper nanoparticles", ACS Nano. 6(3), 2157-2164 (2012). http://dx.doi.org/10.1021/nn300445d

[26] Y. Yin, R. M. Rioux, C. K. Erdonmez, S. Hughes, G. A. Somorjai and A. P. Al ivisatos, "Formation of hollow nanocrystals through the nanoscale Kirkendall effect", Science 304, 711-714 (2004). http://dx.doi.org/10.1126/science.1096566

[27] W. Li, A. Shavel, R. Guzman, J. Rubio-Garcia, C. Flox, J. Fan, D. Cadavid, M. Ibáñez, J. Arbiol, J. R. Morante and A. Cabot, "Morphology evolution of $Cu_{2-x}S$ nanoparticles: from spheres to dodecahedrons", Chem. Commun. 47(37), 10332-10334 (2011). http://dx.doi.org/10.1039/c1cc13803k

[28] C. M. Hessel, M. R. Rasch, J. L. Hueso, B. W. Goodfellow, V. A. Akhavan, P. Puvanakrishnan, J. W. Tunnel

and B. A. Korgel, "Alkyl passivation and amphiphilic polymer coating of silicon nanocrystals for diagnostic imaging", Small 6(18), 2026-2034 (2010). http://dx.doi.org/10.1002/smll.201000825

[29] Z.Chen, Q.Wang, H.Wang, L.Zhang, G.Song, L.Song, J.Hu, H.Wang, J.Liu, M.Zhu and D. Zhao, "Ultrathin PEGylated $W_{18}O_{49}$nanowires as a new 980 nm-laser-driven photothermal agent for efficient ablation of cancer cells *in vivo*", Adv. Mater. 25(14), 2095-2100 (2013). http://dx.doi.org/10.1002/adma.201204616